Linear and Bent Oxo-Bridged Dimers of Ruthenium Pyrazole Nitrosyls

D. Scott Bohle*[a] and Elizabeth S. Sagan[a]

Dedicated to Professor Heinrich Vahrenkamp on the occasion of his 60th birthday

Keywords: Pyrazole complexes / Nitrosyl complexes / Oxo-bridged complexes / Ruthenium / N ligands

The nitrosylation of $RuCl_3 \cdot (H_2O)_x$ in thionyl chloride affords anhydrous $[RuCl_3(NO)]$ which, when treated with a variety of ligands L, gives $[RuCl_3(L)_2(NO)]$. For L = 3,5-dimethylpyrazole (dmpH) it is possible to isolate and characterize the corresponding monomeric complex **1** as well as unusual oxo-bridged dimeric products with nitrosyl ligands *trans* to the oxo ligand with either a linear geometry, as in *trans*-$O[RuCl_2(NO)(dmpH)_2]$ **(2)** and $[Cl_4(NO)Ru]O[Ru(NO)(dmpH)_4]$ **(4)**, or with a bent geometry, as in *trans*-$O[RuCl(NO)(dmpH)(\mu\text{-dmp})]_2$ **(3)**. These compounds have been characterized by elemental analysis and vibrational and NMR spectroscopy, as well as by single crystal X-ray diffraction. Collectively the structural and spectroscopic data support a delocalized π-bonding model across the linear ON–Ru–O–Ru–NO framework.

Introduction

Although ruthenium is renowned for its propensity to form robust adducts of nitric oxide,[1] the majority of these compounds contain relatively soft ligands which favor low formal oxidation states. Thus, to the best of our knowledge there are no reported examples of ruthenium nitrosyl complexes with either terminal oxo or nitrido ligands. Even the number of such complexes where the oxygen or nitrogen atom bridges two centers is very small,[2,3] and there has been surprisingly little research into this area of chemistry. The recognition of the critical role nitric oxide has in biological signal transduction,[4,5] and the increasingly frequent observed interaction of iron proteins with nitric oxide,[6] spur considerable current interest in its coordination chemistry. Nitrosyl derivatives of the oxo-bridged diiron proteins, and related model iron or ruthenium compounds, is a surprisingly sparse area of chemistry and many issues of their stereochemistry, electronic structure, and spectroscopy need to be examined in detail. Herein we describe: (i) the facile synthesis of several examples of mononuclear and oxo-bridged dinuclear ruthenium pyrazole complexes; (ii) the X-ray diffraction structures of three of these derivatives which contain both linear and bent Ru−O−Ru bonds; and (iii) the characterization of these new derivatives. Taken together these results allow us to assess the degree of synergistic π-acceptance and π-donation across the ON−Ru−O−Ru−NO framework.

Results and Discussion

A common synthon in ruthenium(II) nitrosyl chemistry is "$RuCl_3(NO)$" which is readily obtained by passing NO through alcoholic solutions of $RuCl_3 \cdot (H_2O)_x$.[7] Although this solid can be isolated as a trihydrate, it is frequently used directly for reactions with excess ligands L (L = tertiary phosphanes and arsanes, thioethers, or selenyl ethers)[8−10] to give the diamagnetic complexes $[RuCl_3(NO)L_2]$ [Equation (1)]. In these cases the $[RuCl_3(NO)L_2]$ product can usually be isolated in high yield by simple filtration of the product from the ethanol solution; there are no reports of other hydrated or oxo-bridged products being isolated from this one-pot approach. With amines and nitrogen bases this strategy has considerably less general utility; for example, although pyridine, acetonitrile, 2,2′bipyridine, and 1,10-phenanthroline add to $[RuCl_3(NO)]$ to give six-coordinate products, the reaction with ammonia, 3,5-dimethylpyrazole or {[tris(3,5-dimethylpyrazolyl)borate]$^-$ = DMTPZ} under the conditions in Equation 1 leads to mixtures of products and low general yields of the desired product.[8,11] In the case of 3,5-dimethylpyrazole this is due to the formation of the oxo-bridged diruthenium products to be described below. In the case of DMTPZ, however, the low yields (ca. 9%) for $[(DMTPZ)RuCl_2(NO)]$ isolated from the reaction of commercial $[RuCl_3(NO)]$ and Tl(DMTPZ), are in part due to hydrolysis of the DMTPZ to give mono-pyrazole complexes such as **1** in 14% yield.[11]

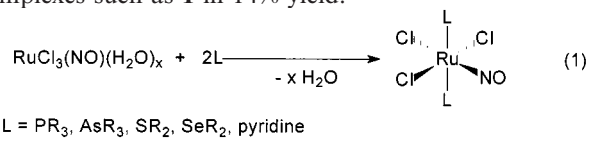

(1)

L = PR_3, AsR_3, SR_2, SeR_2, pyridine

A simple solution to these problems is to dehydrate $RuCl_3 \cdot (H_2O)_x$ by performing the nitrosylation reaction in thionyl chloride. To this end we have modified a method devised by Demant et al. where $RuCl_3 \cdot (H_2O)_x$ is nitrosylated in thionyl chloride [Equation (2)] and the resulting product is filtered off and used directly.[12] When anhydrous $[RuCl_3(NO)]$ is prepared in this manner, and then treated

[a] Department of Chemistry University of Wyoming,
Laramie, WY 82071−3838, USA
Fax: (internat.) + 1-307/766-2807
E-mail: bohle@uwyo.edu

  1434−1948/00/0707−1609 $ 17.50+.50/0

with excess 3,5-dimethylpyrazole in toluene at reflux [Equation (3)], the major product is *mer*-$[RuCl_3(NO)(dmpH)_2]$ **(1)**, which is isolated in 87% yield after chromatography on silica. This product is identical by IR and NMR spectroscopy to that isolated in low yield by Onishi.[11] A trace second product of this reaction is the known bright yellow $[RuCl_3(dmpH)_3]$.[13−15]

$$RuCl_3(H_2O)_x \xrightarrow[-\,x\,SO_2,\,-\,2x\,HCl]{NO,\ SOCl_2(solvent)} RuCl_3(NO) \qquad (2)$$

$$RuCl_3(NO) \xrightarrow[\Delta,\ T = 105\ ^\circ C,\ 22\ h]{2LH,\ toluene} \mathbf{1} \qquad (3)$$

LH = 3,5-dimethylpyrazole

The brick red mononuclear complex **1** has a relatively labile coordination sphere as it is readily converted into a range of other derivatives by hydrolysis or by treating it with an excess of a coordinating ligand, i.e. the reaction of **1** and triphenylphosphane in ethanol at reflux gives $[RuCl_3(NO)(PPh_3)_2]$ in high yield. When **1** is heated to reflux in wet benzene it rapidly hydrolyzes to give mainly the golden colored, oxo-bridged dimer **2** [Equation (4)] and a trace of the oxo and pyrazolato bridged dimer **3**. When **1** is treated with one equivalent of a silver salt there is the rapid formation of a silver chloride precipitate, but the only product isolated from this type of reaction is unchanged starting material, **1**, in ca. 60% yield. Chelating anions such as dibenzyldithiocarbamate also react rapidly with **1** at ambient temperatures to give a mixture of isomers with the formula $[RuCl(Bz_2NCS_2)_2(NO)]$.

$$\underset{\mathbf{1}}{RuCl_3(NO)(LH)_2} \xrightarrow[\Delta,\ T = 76\ ^\circ C]{H_2O,\ (benzene)} \underset{\mathbf{2}}{ON\text{-}Ru\text{-}O\text{-}Ru\text{-}NO} \quad + \mathbf{3}\ (trace) \qquad (4)$$

Under forcing conditions for the reaction of $RuCl_3(NO)\cdot(H_2O)_x$ with 3,5-dimethylpyrazole it is possible to isolate in good yield the mixed μ-oxo; di(μ-pyrazolato) bridged complex, **3** by the addition of excess sodium hydroxide and heating the solution at reflux in ethanol for 16 hours [Equation (5)]. This complex is also formed as a minor product of the synthesis of the linear oxo-bridged complex **2** from the hydrolysis of **1** in benzene. Finally the asymmetric linear complex $[Cl_4(ON)RuORu(NO)(dmpH)_4]$ **(4)** is a minor product of the reaction of thermolyzed $RuCl_3(NO)\cdot(H_2O)_x$ with 3,5-dimethylpyrazole, and can be separated from the major product of this reaction (compound **1**) by column chromatography. Although this product contains formal $16e^-$ and $20e^-$ centers, $\{(ON)RuCl_4\}^{-1}$ and $\{(ON)Ru(dmpH)_4\}^{+3}$, respectively, this distinction rests upon the presence of protons on the 3,5-dimethylpyrazole ligands. In light of the hydrogen bonding observed in the solid state, described below, these formal assignments should not be taken too seriously.

$$RuCl_3(NO)(H_2O)_2 \xrightarrow[EtOH\ \Delta,\ T = 76\ ^\circ C\ 16\ hours]{LH/NaOH} \mathbf{3} \qquad (5)$$

4

Single crystal X-ray crystallography has been used to characterize these derivatives: critical crystallographic parameters are collected in Table 1, views of the four molecules are shown in Figure 1−4, and selected geometrical parameters are collected in Table 2. With the exception of the disordered solvent in **2** the bond lengths and angles are determined precisely and allow for meaningful comparisons. In each case the Ru−NO fragments are linear with short metal−nitrogen bond lengths and a ruthenium geometry close to an ideal octahedron. Overall the ruthenium chloride bonds in these compounds have similar lengths, with the exception of Ru−Cl(1) in **1**, where the chloride *trans* to the nitrosyl is significantly shorter than the others. On average the ruthenium−nitrogen distances to the pyrazole ligands are similar for the terminal pyrazoles, which in turn are slightly longer than the bridging pyrazoles in **3**. This trend is also seen in $[\{(p\text{-cymene})Ru(\mu_2\text{-}OH)\}_2(\mu\text{-pyrazolato})]BF_4$ where the ruthenium−nitrogen bond lengths are 2.078(3) Å.[16]

As can be seen from the ORTEP representations of **2, 3**, and **4** in Figure 1−4 the planes defined by the pyrazole rings adopt an orientation which allow for relatively short N−H···Cl interactions in the solid state. In particular the linear, oxo-bridged dimers have short chlorine−hydrogen interactions: compound **2** has Cl(1)−HN(6) = 2.398(4) Å, Cl(2)−HN(8) = 2.392(4) Å, Cl(3)−HN(2) = 2.435(3) Å, and Cl(4)−HN(4) = 2.371(4) Å, while **4** has Cl(1)−HN(4) = 2.397(2) Å, Cl(2)−HN(6) = 2.330(2) Å, Cl(3)−HN(10) = 2.392(4) Å, and Cl(4)−HN(8) = 2.354(2) Å. On the other hand, in the mononuclear complex **1** and the bent oxo-bridged dimer **3**, the chloride−hydrogen separations are much longer; in **1** Cl(1)−HN(3) = 2.748(2) Å, and Cl(2)−HN(5) = 2.690(4) Å, while in **3** these separations are Cl(1)−HN(10) = 2.757(2) Å, and Cl(2)−HN(8) = 2.791(3) Å. Correlated with these structural observations are variations in the frequencies of the N−H stretching bands, ν(N−H) between 3598 cm^{-1} in **4** to 3140 cm^{-1} in **2**.

Characteristic vibrational and electronic spectroscopic data for these compounds are collected in Table 3. The nitrosyl stretching frequencies clearly fall into the region for linear nitrosyls, and all of the oxo-bridged dimers

Table 1. Crystallographic data and refinement parameters

Compound	**1**	**2**	**3**	**4**
Empirical formula	$C_{10}H_{16}Cl_3N_5ORu$	$C_{20}H_{32}N_{10}Cl_4O_3Ru_2{\cdot}C_2H_5OH$	$C_{20}H_{30}N_{10}Cl_2O_3Ru_2$	$C_{20}H_{32}N_{10}Cl_4O_3Ru_2$
Mass (g mol^{-1})	429.7	849.63	731.58	804.56
Color; Habit	Red; Block	Orange; Prism	Burgundy; Prism	Orange; Prism
Crystal size (mm)	0.58 × 0.22 × 0.1	0.45 × 0.36 × 0.04	1.26 × 0.46 × 0.36	0.48 × 0.20 × 0.12
Crystal system	Monoclinic	Monoclinic	Monoclinic	Monoclinic
Space group	$P2_1/n$	$C2/c$	$P2_1/n$	$P2_1/c$
a (Å)	12.103(2)	37.41(1)	10.407(2)	16.250(2)
b (Å)	11.088(2)	10.665(3)	19.166(5)	10.640(1)
c (Å)	12.641(2)	18.911(5)	15.240(3)	19.637(4)
β (°)	109.50(2)	112.46(1)	108.14(1)	96.67(1)
Volume (Å ^{3})	1599.1(4)	6972(4)	2889(1)	3372.3(7)
Z	4	8	4	4
Density (Mg m^{-3})$_c$	1.785	1.609	1.682	1.752
μ (mm^{-1})	1.483	1.215	1.271	1.412
22 Range (°)	4.04 to 50.00	4.0 to 50.0	3.5 to 50.0	4.2 to 50.0
Index ranges h	$-1 \le h \le 14$	$-44 \le h \le 1$	$-1 \le h \le 12$	$-1 \le h \le 19$
k	$-1 \le k \le 13$	$-11 \le k \le 1$	$-1 \le k \le 22$	$-1 \le k \le 12$
l	$-15 \le l \le 14$	$-18 \le l \le 20$	$-18 \le l \le 17$	$-23 \le l \le 23$
Obs. Reflections	2814	4515	5081	5920
Final R (obs.)	$R = 0.032$	$R = 0.067$	$R = 0.046$	$R = 0.037$
	$R_w = 0.086$	$R_w = 0.178$	$R_w = 0.121$	$R_w = 0.095$
Goodness-of-fit	1.03	0.987	1.085	1.065
Data-to-parameter ratio	15.5:1	12.0:1	15.2:1	15.6:1
Largest diff. peak	0.58 e Å^{-3}	1.41 e Å^{-3}	0.84 e Å^{-3}	0.75 e Å^{-3}
Largest diff. hole	−0.72 e Å^{-3}	−1.18 e Å^{-3}	−1.3 e Å^{-3}	−1.1 e Å^{-3}

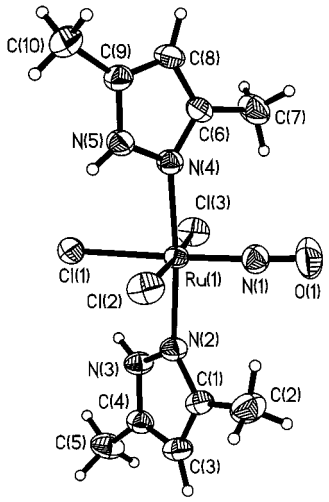

Figure 1. ORTEP view of $[RuCl_3(NO)(dmpH)_2]$ **(1)** showing all hydrogen atoms in calculated positions and all heavy atoms as 30% thermal ellipsoids

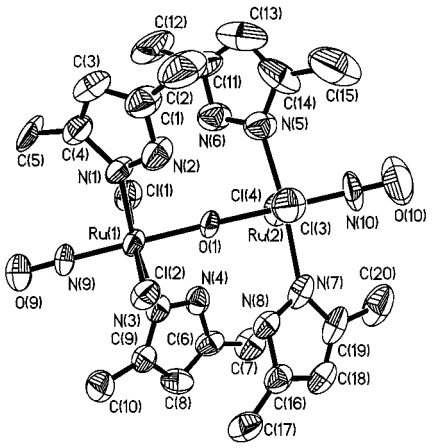

Figure 2. ORTEP view of $O[RuCl_2(NO)(dmpH)_2]_2$ **(2)** showing non-hydrogen atoms as 30% thermal ellipsoids

2−4 have lower ν(NO) frequencies than does the mononuclear complex **1**. In the case of complex **2** there is a single, strong and relatively broad ν(NO) band at 1809.1 cm^{-1} in the infrared spectrum and this is assigned as the asymmetric nitrosyl stretch across the ON−Ru−O−Ru−NO framework. In the Raman spectrum a single weak band at slightly higher energy (1821 cm^{-1}) is observed for **2**, and this is assigned as a symmetric nitrosyl stretch for the dinuclear framework. For complexes **3** and **4** both ν(NO) modes are IR active and in both cases are split by ca. 28 cm^{-1}, a value significantly higher than found for **2**. The similarity in splitting is somewhat surprising in light of the different ruthenium environments in the case of **4** and the C_2 symmetry present in **3**. The Ru−O−Ru framework also has a strong IR active ν(Ru−O−Ru)$_{asym}$ at 791.7 cm^{-1} as well as a Raman active ν(Ru−O−Ru)$_{sym}$ mode at 334 cm^{-1} for the linear dimer **2**. As shown in Figure 5, the low energy Raman spectra for **1−4** contain numerous common bands including a strong band 589−602 cm^{-1} and weaker bands at 441−448 cm^{-1}, 359−365 cm^{-1}, and 282−291 cm^{-1}. For the bent oxo-bridged dimer **3** there is a unique weak band at 495 cm^{-1} which may be due to either the ν(Ru−O−Ru)$_{sym}$ band or to the bridging pyrazole. In **4** it is difficult to assign a unique band to the ν(Ru−O−Ru)$_{sym}$ mode.

The electronic spectra for the oxo-bridged dimers are dominated by three bands, with the lowest energy band being relatively weak and broad and generally observed as a shoulder to the stronger UV bands. For the oxo-bridged dimer **3**, the two most prominent UV bands are at lower energies than for either of the linear oxo-bridged dimers **2** or **4**. For the mononuclear complex **1** the intense red color

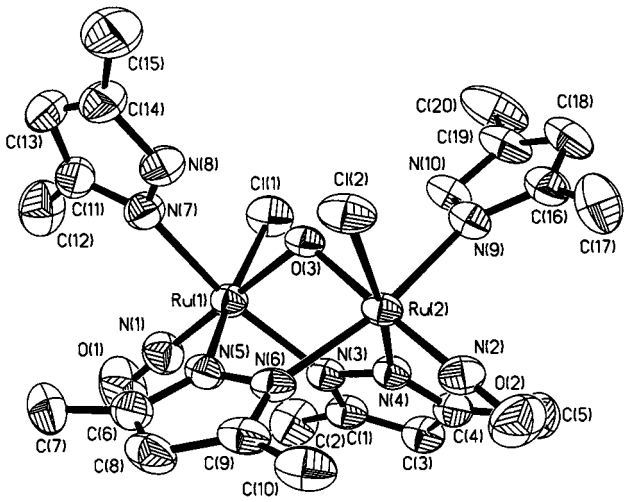

Figure 3. ORTEP view of $O[RuCl_2(NO)(dmpH)(dmp)]_2$ **(3)** with non-hydrogen atoms represented as 30% thermal ellipsoids

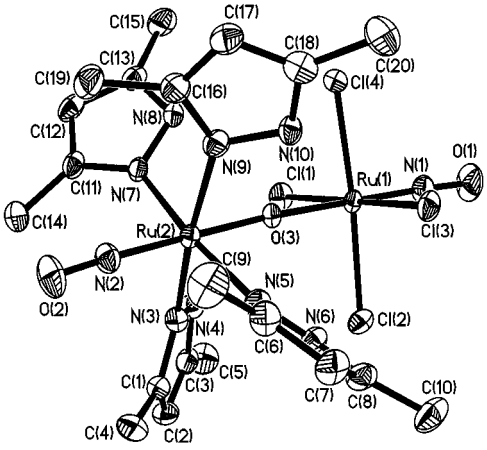

Figure 4. ORTEP view of $[Cl_4(NO)Ru]O[Ru(NO)(dmpH)_4]$ **(4)** with hydrogen atoms omitted and all other atoms represented as 30% thermal ellipsoids

is due to a comparatively strong low energy band at 538 nm. All of the new complexes described in this paper are clearly diamagnetic at room temperature and give sharp ^1H and ^{13}C NMR spectra with no indication of fluxional exchange broadening. In each case the solution spectra indicate that the structures determined by X-ray diffraction correspond to those in solution. The electrochemistry of species **1**−**4** is dominated by irreversible reductions at circa −0.9 V. In the cyclic voltammetry experiments no return wave is seen, even at relatively fast sweep rates (2000 mV s^{-1}) and the oxidative sweep indicates numerous new by-products from these processes.

There are surprisingly few well-characterized metallonitrosyl complexes with either bridging or terminal oxo ligands. This might be attributable to the widely perceived notion that the oxo ligand and strong π-accepting ligands such as a nitrosyl have differing preferences for a metal's oxidation state and environment. In terms of group 8 transition metals there are several early reports of oxo-bridged ruthenium nitrosyl dimers $Ru_2N_6O_{15}$ stemming from the addition of nitric oxide to RuO_4.[2,3] More recently, an oxo-bridged osmium porphyrin nitrosyl complex has been serendipitously isolated and structurally characterized from the reaction of [Os(OEP)(CO)] and ClNO.[17] Other examples of the ON−M−O−M−NO framework can be found for Ir, μ_2-$O[Ir(NO)(PPh_3)_2]_2$,[18,19] and its oxidative-addition products,[20,21] as well as more numerously for molybdenum.[22−25] In general the iridium examples are similar to those described here for ruthenium in the that the nitrosyl is *trans* to the oxo-ligand, while in the case of molybdenum the nitrosyls are *cis* to the oxo bridge. This trend may be due to the use of polyhapto chelate ligands in the molybdenum examples; in these cases the ancillary ligand is required to occupy the *trans* position. It remains an open question whether an oxo-bridged molybdenum nitrosyl dimer with a less constrained coordination sphere would

Table 2. Selected geometric parameters for crystallographically characterized compounds

	$RuCl_3(NO)(LH)_2$ **1**	$O[RuCl_2(NO)(LH)_2]_2$ **2**	$O[RuCl(LH)(\mu_2\text{-}L)(NO)]_2$ **3**	$O[RuCl_4(NO)][Ru(LH)_4(NO)]$ **4**
Ru−O (Å)		Ru(1) 1.917(6) Ru(2) 1.885(6)	Ru(1) 1.910(3) Ru(2) 1.913(3)	Ru(1) 1.940(2) Ru(2) 1.873(2)
Ru−O−Ru (°)		178.9(4)	116.35(13)	176.6(2)
O−Ru−NO (°)		Ru(1) 179.6(4) Ru(2) 179.0(4)	Ru(1) 178.1(2) Ru(2) 178.2(2)	Ru(1) 177.67(14) Ru(2) 179.27(14)
Ru−NO (Å)	1.735(3)	Ru(1) 1.734(9) Ru(2) 1.721(10)	Ru(1) 1.747(4) Ru(2) 1.752(4)	Ru(1) 1.731(3) Ru(2) 1.759(3)
Ru−N−O (°)	177.5(3)	Ru(1) 178.5(10) Ru(2) 177.1(13)	Ru(1) 177.7(5) Ru(2) 179.6(4)	Ru(1) 176.2(3) Ru(2) 177.0(3)
Ru−Cl (Å)	Cl(1) 2.3389(9) Cl(2) 2.3625(9) Cl(3) 2.3812(9)	Cl(1) 2.388(3) Cl(2) 2.369(3) Cl(3) 2.381(4) Cl(4) 2.371(4)	Cl(1) 2.3978(13) Cl(2) 2.3988(11)	Cl(1) 2.385(1) Cl(2) 2.398(1) Cl(3) 2.401(1) Cl(4) 2.377(1)
Ru−N_{pz} (Å)	N(2) 2.096(3) N(4) 2.102(3)	N(1) 2.087(9) N(3) 2.067(10) N(5) 2.090(10) N(7) 2.090(10)	N(3) 2.074(4) N(4) 2.058(3) N(5) 2.064(4) N(6) 2.061(4) N(7) 2.095(4) N(9) 2.102(4)	N(3) 2.081(3) N(5) 2.085(3) N(7) 2.082(3) N(9) 2.080(3)

Table 3. Characteristic spectroscopic data for key compounds

Compound	Vibrational bands[a] ν(NO)	ν(NH)	ν(RuORu)	Electronic bands nm(log{ε})
1	1883.4 (s) IR	3387.8 (m) 3329.9 (m)	–	538 (1.77) 430 (189) 296 (3.36) 264 (3.34)
2	1809.1 (s) IR 1821 (w) RA	3219.0 (m) 3140 (m)	791.7 (s) IR 744 (m) RA	520 (shoulder) 343 (4.35) 264 (3.95)
3	1829.4 (s) IR 1802.4 (s) IR 1821 (m) RA 1795 (w) RA	3208.4 (m)	715.5 (s) IR 680.9 (m) RA	520 (2.50) 396 (3.35) 293 (4.24)
4	1818.2 (s) IR 1790.2 (s) IR	3598 (w) 3248(m)	792.2 (s) IR 786.1 (m) RA	450 (shoulder) 343 (4.72) 264 (4.33)

[a] All vibrational frequencies are given in cm^{-1} and measured in KBr for infrared bands (IR) or as a neat powder for the Raman active bands (RA).

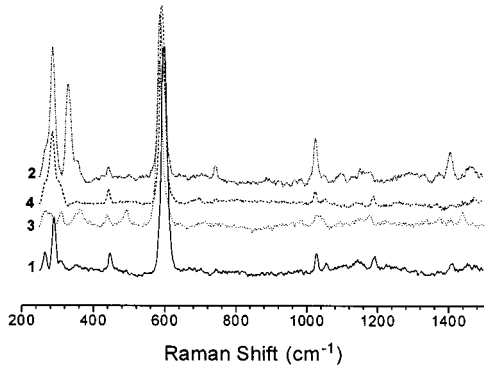

Figure 5. Raman spectra of compounds **1**–**4** measured as powders with 648 nm excitation radiation; **1** (bottom, solid line), **2** (top, dash double dotted line), **3** (second from bottom, dotted line ·····), and **4** (dashed line)

adopt a *cis* or *trans* oxo geometry. Thus there is little intrinsically incompatible with coordination of oxo and nitrosyl ligands within a single coordination sphere.

Attempts to prepare sulfur-bridged analogues to **2**–**4** have been unsuccessful. Thus when **1** is treated with hydrogen sulfide under the conditions which lead to hydrolytic dimerization to give **2**, there is rapid formation of an amorphous black powder that is completely insoluble in most solvents. This solid still contains a strong sharp nitrosyl stretching band at 1785 cm^{-1} in the IR and analyzes for RuS_4NO contaminated with some pyrazole species. Thus, excess hydrogen sulfide results not only in the loss of the *trans* chloride in **1**, but also the two remaining chlorides and the two 3,5-dimethylpyrazole ligands. In an attempt to control the stoichiometry of the sulfur substitution reaction more carefully, compound **1** was treated with $S(SiMe_3)_2$ in benzene at reflux. However under these conditions **1** was quantitatively recovered unchanged.

Complexes **2**–**4** have the potential of a "push-pull" in the bonding along the ON–Ru–O–Ru–NO framework. In this overly simplified model the nitrosyls act as π-accepting ligands while the oxo is a π-donor ligand. In higher oxidation states the bridging-oxo ligand is known to mediate strong ruthenium–ruthenium interactions as evidenced by reversible electrochemistry and by the strong coupling observed in the magnetic susceptibility of $[(bipy)_2ClRuORuCl(bipy)_2]^{n+}$ (n = 2 or 3).[26] In the qualitative molecular-orbital scheme proposed by Weaver et al.[26] two *p*-type lone pairs of the oxygen can π–bond with the six t_{2g} orbitals based on the two ruthenium to give pairs of π-bonding, nonbonding, and antibonding orbitals, as well as the two d_{xy} ruthenium orbitals. These π-orbital pairs are degenerate in the linear D_{4h}-symmetric complexes and are closely spaced for D_{2h}-symmetric species such as **2**. Regardless of the local symmetry, this molecular orbital scheme leads to no net stabilizing interaction for ruthenium(II) oxo-bridged dimers since the t_{2g} set is full. This correlates with the general absence of linear oxo-bridged complexes of d^6 metal centers. However, once a nitrosyl ligand is introduced into the *trans* position to the oxo-bridge there will be strong backbonding interactions between the filled π^* and π_{NB} orbitals and the accepting π^* orbitals of the nitrosyl ligands. In a qualitative sense these interactions should be stronger than in the parent complex because the energy match between the π^* and π_{NB} and the π^*_{NO} will be better since the former orbitals are of higher energy. In addition, the overlap between these orbitals will probably increase due to the spatial extension of these orbitals towards the nitrosyl. Thus in these qualitative terms the net π-interaction for the ON–Ru–O–Ru–NO fragment is expected to be highly stabilizing in a linear geometry, and stabilized to a similar extent in a bent Ru–O–Ru geometry.

The structural consequences of possible π-delocalization over the oxo-ruthenium-nitrosyl framework are expected to be manifested most strongly in the trends in the ruthenium–oxygen distances for the bridged oxo ligand. Thus the ruthenium–oxygen bonds in **2**–**4** might be expected to be shorter than those in related complexes which lack a strong π-accepting ligand *trans* to the bridging oxo group. There are few direct comparison complexes where oxo ligands bridge two ruthenium(II) d^6 centers. However there is little significant difference between the two Ru–O bond lengths in linear bridged **2** or **4** and the bent species **3**. There is a significant difference between the

ruthenium−oxygen bond lengths in the asymmetric linear bridged species **4** where the Ru(1)−O(3) for the $RuCl_4(NO)$ group, formally with a −1 charge, is 0.067(2) Å longer than Ru(2)−O(3) for the $Ru(LH)_4(NO)$ group which formally has a charge of +3. Note however that all of these bond lengths are about 0.05 and 0.1 Å longer than the ruthenium−oxygen bond lengths in linear Ru^{III} and Ru^{IV} oxo-bridged dimers found in the CCDB.[27] The Ru−O−Ru bending found in **3** is similar to that found in structurally characterized carboxylato, oxo-bridged ruthenium dimers where the mean ruthenium−oxygen−ruthenium bond angle is 122.3 °.[27]

For the nitrosyl stretching frequencies the formation of the oxo-bridge results in an 80 cm^{-1} decrease in the two ν(NO) bands, and this suggests increased Ru−NO back-bonding in all three of the oxo-bridged complexes. Correlated with this trend are the Ru−O bond lengths which range between 1.873(2) and 1.940(2) Å, values which are ca. 0.20 Å shorter than for the many nonchelating Ru^{II}−OR bond lengths in the CCDB. On the other hand these bond lengths are ca. 0.05−0.1 Å longer than for structurally characterized high-valent, oxo-bridged ruthenium dimers which typically contain electronegative ligands *trans* to the oxo-bridge. The ν(Ru−O−Ru) stretching frequencies for **2**−**4** are also lower than for high-valent species. For example, in $K_4Ru_2OCl_{10}$ $\nu(Ru-O-Ru)_{asym}$ = 888 cm^{-1} and $\nu(Ru-O-Ru)_{sym}$ = 259 cm^{-1}, and have a difference $\nu_{asym}-\nu_{sym}$ = 629 cm^{-1}.[28] For **2** the values are ν_{asym} = 791.7 cm^{-1} and ν_{sym} = 343 cm^{-1}, with a difference $\nu_{asym}-\nu_{sym}$ = 449 cm^{-1}. The ν_{asym} frequency is at the low end of the reported range for these modes, and this correlates with the small difference between the two Ru−O−Ru stretching modes.[29,30]

Although the most well understood receptor for nitric oxide is the heme protein soluble guanylate cyclase,[31,32] a diverse array of other physiological sinks for nitric oxide have been proposed.[33] In many cases the critical protein/nitric oxide interaction is the binding of nitric oxide to enzymatically active metals such as the diiron site in bacterioferritin,[34] the oxo-bridged diiron center in hemerythrin[35] or methane monooxygenase hydroxylase,[36] the [2Fe-2S] iron-sulfur cluster in mammalian ferrochelatase,[37] or the [4Fe-4S] cluster in HiPIP.[38] In these cases the new nitrosylated ferroproteins have markedly different redox, structural, and kinetic properties as compared to the parent protein, and a current major interest in metallobiochemistry is understanding how nitrosylation mediates these effects. For the oxo-bridged diiron proteins, nitrosylation of the iron(s) can potentially result in the introduction of the nitric oxide *cis* or *trans* to the oxo bridge. Although in most cases the specific coordination geometry of these nitrosylated diiron sites is not known, our work suggests that *trans* coordination geometries may be thermodynamically favored.

Conclusion

In all of the chemistry described in this paper the nitrosyl and oxo-ligands retain a rigorous *trans* geometry; there is no indication of either isomerization or the presence of isomers where these two ligands are *cis*. However, other isomers or related complexes may very well be accessible with a judicious choice of conditions or with other ligand sets. The *trans* arrangement of the oxo-bridge and nitrosyl allows for some π-delocalization as evidenced by the spectroscopic and structural results.

Experimental Section

General: The instrumentation, methods, apparatus, and experimental techniques have been described in detail in previous papers.[39] 3,5-Dimethylpyrazole and thionyl chloride were purchased from Aldrich and used as provided. Ruthenium(II)nitrosyl trichloride was either synthesized by a variation of the method of Demant et al.[12] or the solid was purchased from Strem Chemicals. In general the pyrazole complexes are stable towards aerial oxidation and hydrolysis and thus they can be stored, chromatographed, and handled in the open. Electrochemistry experiments were performed with a BAS-50 W potentiostat with a platinum disk electrode, a silver auxiliary electrode, and a silver/silver chloride reference electrode. All experiments were performed in dry oxygen-free dichloromethane at room temperature with 0.1 M $[N(n\text{Bu})_4][PF_6]$ backing electrolyte.

Anhydrous $RuCl_3(NO)$: Commercial hydrated ruthenium trichloride (321 mg) was suspended in 10 mL thionyl chloride in a Fisher−Porter bottle and the vessel flushed with nitrogen before pressurizing with nitric oxide to 2.76 bar (40 psi). This mixture was then heated at 65 °C for 12 hours during which time the original black suspension dissolved to give a deep red solution from which a fine red solid precipitated upon cooling to room temperature. After flushing the head space of the reactor with nitrogen, dry carbon tetrachloride (30 mL) was added and the solution filtered to give 350 mg (95%) of red product. − IR (Nujol): ν(NO) = 1894 cm^{-1}. − Cl_3NORu (237.43): calcd. Cl 44.79, N 5.90; found Cl 44.95, N 5.71.

***mer*-$[RuCl_3(NO)(dmpH)_2]$ (1):** $RuCl_3NO$ (0.07 g), prepared by treating $RuCl_3$ with nitric oxide in thionyl chloride, in dry toluene (20 mL) was treated with 3,5-dimethylpyrazole (1.4 g) at reflux for 22 h. During this period, and upon subsequent cooling, a deep-red precipitate formed, which was filtered and washed with copious quantities (50 mL) of ethanol, and subsequently with water, ethanol, and hexanes. The yield of this crude material, which is mostly **1** and a small quantity of bright yellow $[RuCl_3(dmpH)_3]$, was 122 mg. Final purification was achieved by column chromatography on silica gel (20 cm × 4 cm column, with chloroform as the eluent) to elute first the deep red-purple $[RuCl_3(NO)(dmpH)_2]$, which was recovered in a final yield of 87% (111 mg) by addition of ethanol and concentrating the solution on a rotary evaporator to remove the chloroform. Elution with acetone/chloroform (4:50) gave traces of a bright yellow compound, which was subsequently identified as $[RuCl_3(dmpH)_3]$.[14,15] $RuCl_3(NO)(dmpH)_2$: UV/Vis (CH_2Cl_2): λ_{max} (log ε[M^{-1} cm^{-1}]) = 538 (1.77) nm, 430 (1.89), 296 (3.36), 264 (3.34). − ^1H NMR (22 °C, $CDCl_3$): δ = 10.74 (s, 1 H, N−*H*), 5.99 (s, 1 H, C−*H*), 2.61 (s, 3 H, C*H*$_{3'}$), 2.37 (s, 3 H, C*H*$_{3'}$). − ^{13}C NMR (22 °C, $CDCl_3$) δ = 153.8, 143.1(s, *C*−CH_3), 108.0(s, *C*−H), 14.7, 11.4 (s, C−*C*H_3). − IR (KBr): ν(NH) = 3387.8 (m) cm^{-1}, 3329.9 (m); ν(NO) = 1883.4 (s); with additional bands at 1569 (m), 1276.8 (m), 1186.2 (w), 1157.3 (w), 1056.9 (m), 823.6 (w), 792.7 (m), 655.8 (m), 569 (w), 505.3 (m) cm^{-1}. − $C_{10}H_{16}Cl_3N_5ORu$

(429.73): calcd. C 27.95, H 3.75, N 16.30; found C 28.15, H 3.95, N 16.10. − M.p. 248 °C(dec). This complex is also a by-product of the addition of 3,5-dimethylpyrazole to the direct nitrosylation product of $RuCl_3{\cdot}(H_2O)_x$ in ethanol, followed by chromatographic separation. Crystals suitable for X-ray diffraction were grown by vapor-phase diffusion of 2-propanol into a chloroform solution of **1** at −20 °C.

***trans*-O[RuCl$_2$(NO)(dmpH)$_2$] (2):** $RuCl_3(NO)(dmpH)_2$ (**1**; 41 mg) in 20 mL (wet) benzene was heated at reflux for 16 hours in the open air. The resulting red-orange solution was cooled and the benzene removed on a rotary evaporator. The red crystalline solid was taken up in dichloromethane and chromatographed on a 30 × 2 cm silica column with dichloromethane. The first yellow-orange fraction was collected and recrystallized by the addition of an equal volume of ethanol and concentration to 20 mL. The resulting flaky orange-yellow solid was filtered and washed with ethanol and hexane and dried to give **2** (32 mg, 83%). Further elution of the column with dichloromethane gave 5 mg of the bent oxo-pyrazolato complex **3**. − UV/Vis (CH_2Cl_2): λ_{max} (log ε[M^{-1} cm^{-1}]) = 520 (shoulder) nm, 343 (4.35), 264 (3.95). − ^{1}H NMR (22 °C, $CDCl_3$): δ = 12.15 (s, 1 H, N-*H*), 5.67 (d, $^4J_{HH}$ = 1.14 Hz, 1 H, C−*H*), 2.59, 2.05 (s, 3 H, C$H_{3'}$). − ^{13}C NMR (22 °C, $CDCl_3$): δ = 151.2, 142.4 (s, *C*−CH_3), 106.3 (s, *C*−H), 14.0, 10.7(s, C−*C*H_3). − IR (KBr): ν(NH) = 3219 (s) and 3140 (w) cm^{-1}; ν(NO) = 1809.1 (s); $\nu(RuORu)_{as}$ = 791.7 (s); with additional bands at 1570.9 (m), 1473.4 (w), 1409.9 (m), 1377.1 (w), 1276.8 (m), 1191.9 (m), 1151.4 (w), 1056.9 (m), 746.4 (w), 690.5 (m), 582.5 (m), 446.5 (w) cm^{-1}. − $C_{20}H_{32}Cl_4N_{10}O_3Ru_2$ (804.56): calcd. C 29.86, H 4.01, N 17.41; found C 30.08, H 4.01, N 17.32. Crystals suitable for X-ray diffraction were grown by vapor-phase diffusion of ethanol into a dichloromethane solution of **2**.

***trans*-O[RuCl(NO)(dmpH)(μ-dmp)]$_2$ (3):** In a 100 mL Fisher−Porter pressure bottle $RuCl_3{\cdot}(H_2O)_x$ (0.118 g) was suspended in 30 mL absolute ethanol and sealed with a stainless steel pressure head. The solution and apparatus was purged for 30 minutes with a stream of nitrogen and then pressurized with 2.76 bar (40 psi) of nitric oxide at ambient temperature. After 5 hours the pressure was brought back to 2.76 bar (40 psi) and the mixture was allowed to stir for a total of 20 hours at room temperature during which time the color changed from a deep red-black to pink. Following the release of NO pressure the solution and apparatus was purged for an additional 40 minutes with a stream of nitrogen and the uniform ethanol solution of "$RuCl_3(NO)$" was transferred to a 100 mL round bottom flask to which was added 3,5-dimethylpyrazole (2.5 equiv., 0.137 g) and sodium hydroxide (1 equiv., 0.023 g) in 1 mL water. The resulting darkened solution was heated at reflux for 16 hours and then cooled to give a copious deep red precipitate of product. After filtration and successive washes with ethanol, water, and ethanol the burgundy-colored product was dried in a vacuum desiccator. Recrystallization from dichloromethane/ethanol gave **3** (0.124 g, 61%). − UV/Vis (CH_2Cl_2): λ_{max} (log ε[M^{-1} cm^{-1}]) = 520 (2.50) nm, 396 (3.35), 293 (4.24). − ^{1}H NMR (22 °C, $CDCl_3$): δ = 11.87 (s, 1 H, N−*H*), 5.88 and 5.73 (s, 1 H, C−*H*), 2.59, 2.58, 2.17, and 2.06 (s, 3 H, C$H_{3'}$). − ^{13}C NMR (22 °C, $CDCl_3$): δ = 152.9, 142.7 [s, *C*−CH_3(pyrazole)], 150.8 [s, *C*−CH_3(pyrazolate)], 108.5 and 107.2 (s, *C*−H), 14.6, 11.3 [s, C−*C*H_3(pyrazole)], 13.7, 13.8 [s, C−*C*H_3(pyrazolate)]. − IR (KBr): ν(NH) = 3208.4 (m); ν(NO) = 1829.4 (s) and 1802.4 (s); $\nu(RuORu)_{as}$ = 715.5 (s) cm^{-1}; with additional bands at 1565.1 (m), 1534.3 (w), 1473.4 (m), 1444.6 (m), 1419.5 (s), 1380 (m), 1353 (w), 1271 (m), 1187.1 (m), 1148.5 (m), 1016.3 (m), 788.8 (m), 775.3 (m), 649 (w), 580.5 (m), 496.6 (w), 440.7 (w) cm^{-1}. − $C_{20}H_{30}Cl_2N_{10}O_3Ru_2$ (731.64): calcd. C 32.84, H 4.13, N 19.15; found C 32.96, H 4.17, N 19.10. Crystals suitable for X-ray diffraction were grown by vapor-phase diffusion of ethanol into a dichloromethane solution of **3**.

[Cl$_4$(NO)Ru]O[Ru(NO)(dmpH)$_4$] (4): Hydrated ruthenium trichloride (1.1 g) was suspended in 50 mL ethanol in a 100 mL Fisher−Porter bottle, and was nitrosylated with 2.76 bar (40 psi) of nitric oxide pressure for 20 hours. During this period the initially black-red suspension became a uniform pale red color. After releasing the excess nitric oxide pressure and flushing the solution with nitrogen, the pale-red solution was transferred to a 100 mL round bottom flask and the solvent removed at room temperature. The resulting solid was heated to 86 °C under a water aspirator vacuum for 45 minutes and the red-black residue was then taken into an inert atmosphere box under nitrogen. This solid was suspended in 30 mL dry ethanol and allowed to react with 3,5-dimethylpyrazole (1.53 g) for 3 hours at reflux. This solution was cooled to room temperature to give a copious red precipitate and a black solution, which was then filtered and washed with ethanol and hexane to give 1.39 g of red solid. This crude product was a mixture of **1**, **2**, **3**, and **4**, which was separated by column chromatography on silica gel (20 × 5 cm column) with dichloromethane used to elute **1** (69%) and **2**(18%). Chloroform was used to elute **3** (trace) as a purple band, which was followed by a slow moving orange band **4**. The asymmetrical linear oxo-bridged product was separated by eluting with 5:1 chloroform/acetone and isolated by the addition of 20 mL ethanol followed by concentration and crystallization on the rotary evaporator. Filtration followed by successive washes with ethanol and hexane gave 25 mg (12%) of red-orange crystals UV/Vis (CH_2Cl_2): λ_{max} (log ε[M^{-1} cm^{-1}]) = 450 (shoulder) nm, 343 (4.72), 264 (4.33). − ^{1}H NMR (22 °C, $CDCl_3$): δ = 12.49 (s, 1 H, N−*H*), 5.91(s, 1 H,C−*H*), 2.39, 1.93 (s, 3 H, C$H_{3'}$). − ^{13}C NMR (22 °C, $CDCl_3$): δ = 150.6, 145.3 (s, *C*−CH_3), 107.1 (s, *C*−H), 12.8, 11.8 (s, C−*C*H_3). − IR (KBr): ν(NH) = 3598 (w), and 3148 (m) cm^{-1}; ν(NO) = 1818.2 (s) and 1790.2 (s); $\nu(RuORu)_{as}$ = 792.2 (s); with additional bands at 1569.9 (m), 1473 (w), 1409.3 (m), 1376 (w), 1284.4 (m), 1184.2 (m), 1060.2 (m), 711.6 (m), 655.2 (w), 579.5 (m) cm^{-1}. − $C_{20}H_{32}Cl_4N_{10}O_3Ru_2$ (804.56): calcd. C 29.86, H 4.01, N 17.41; found C 29.69, H 4.24, N 17.12. Crystals suitable for X-ray diffraction were grown by vapor-phase diffusion of ethanol into a dichloromethane solution of **4**.

X-ray Crystallographic Study

X-ray diffraction data were collected at room temperature for single crystals of compounds $[RuCl_3(NO)(dmpH)_2]$ **(1)**, $[O\{RuCl_2(NO)(dmpH)_2\}_2]$ **(2)**, $[O\{RuCl_2(NO)(dmpH)(\mu\text{-}dmp)\}_2]$ **(3)**, and $[Cl_4(ON)RuORu(NO)(dmpH)_4]$ **(4)** on a Siemens P4 Diffractometer equipped with a molybdenum tube [$\lambda(K_{\alpha 1})$ = 0.70926 Å; $\lambda(K_{\alpha 2})$ = 0.71354 Å] and a graphite monochromator. In each case the diffraction data were measured using ω scans. The intensities of three standard reflections monitored every 100 reflections during the respective data collections indicated negligible crystal decomposition. The structures were solved by direct methods and refined by full-matrix least-squares techniques on F^2 using structure solution programs from the SHELXTL program.[40] Important crystallographic parameters are collected in Table 1.

Crystallographic data (excluding structure factors) for the structure(s) reported in this paper have been deposited with the Cambridge Crystallographic Data Centre as supplementary publication no. CCDC 139381−139384, for **1**−**4** respectively. Copies of the data can be obtained free of charge on application to CCDC, 12

Union Road, Cambridge CB2 1EZ, UK [Fax: (internat.) + 44-1223/336-033; E-mail: deposit@ccdc.cam.ac.uk].

Acknowledgments

We gratefully acknowledge financial support from the DOE, (Grant DE-FCO2−91ER) and Professor Keith Carron of this department for the generous use of his laser Raman spectrometer.

[1] W. P. Griffith, *The Chemistry of the Rarer Platinum Metals*, Interscience Publishers, New York, **1967**.
[2] D. Scargill, J. M. Fletcher, *Proc. Chem. Soc. (London)* **1961**, 251.
[3] F. S. Matrin, J. M. Fletcher, P. G. M. Brown, B. M. Gatehouse, *J. Chem. Soc.* **1959**, 76.
[4] R. F. Furchgott, *Angew. Chem. Int. Ed.* **1999**, 38, 1871−1880.
[5] I. J. Ignarro, *Angew. Chem. Int. Ed.* **1999**, 38, 1882−1892.
[6] S. Pfeiffer, B. Mayer, B. Hemmens, *Angew. Chem. Int. Ed.* **1999**, 38, 1715−1731.
[7] J. M. Fletcher, I. L. Jenkins, F. M. Lever, F. S. Martin, A. R. Powell, R. Todd, *Inorg. Nucl. Chem.* **1955**, 1, 378−401.
[8] M. B. Fairy, R. J. Irving, *J. Chem. Soc. (A)* **1966**, 475−479.
[9] R. E. Townsend, K. J. Coskran, *Inorg. Chem.* **1971**, 10, 1661−1664.
[10] J. E. Fergusson, C. T. Page, *Aust. J. Chem.* **1976**, 29, 2159−2165.
[11] M. Onishi, *Bull. Chem. Soc. Jpn.* **1991**, 64, 3039−3045.
[12] U. Demant, W. Willing, U. Muller, K. Dehnicke, *Z. Anorg. Allg. Chem.* **1986**, 532, 175−183.
[13] J. Soucek, *Coll. Czech. Chem. Commun.* **1962**, 27, 1645−1650.
[14] F. Kralik, J. Vrestal, *Coll. Czech. Chem. Commun.* **1962**, 27, 1651−1657.
[15] F. Kralik, J. Vrestal, *Coll. Czech. Chem. Commun.* **1961**, 26, 1298−1304.
[16] D. Carmona, A. Mendoza, J. Ferrer, F. J. Lahoz, L. O. Oro, *J. Organometal. Chem.* **1992**, 431, 87−102.
[17] L. Cheng, C. Li, H.-S. Chung, M. A. Khan, G. B. Richter-Addo, *Organometallics* **1998**, 17, 3853−3864.
[18] P. Carty, A. Walker, M. Mathew, G. J. Palenik *J. Chem. Soc., Chem. Commun.* **1969**, 1374−1375.
[19] G. S. Brownlee, P. Carty, D. N. Cash, A. Walker, *Inorg. Chem.* **1975**, 14, 323−327.
[20] F. W. B. Einstein, D. Sutton, P. L. Vogel, *Inorg. Nucl. Chem. Lett.* **1976**, 12, 671−675.
[21] P.-T. Cheng, S. C. Nyburg, *Inorg. Chem.* **1975**, 14, 327−329.
[22] H. Adams, N. A. Bailey, G. Denti, J. A. McCleverty, J. M. A. Smith, A. Wlodarczyk, *J. Chem. Soc., Dalton Trans.* **1983**, 2287−2292.
[23] D. Sellmann, B. Seubert, F. Knock, M. Moll, *Z. Anorg. Allg. Chem.* **1991**, 600, 95−108.
[24] P. Legzdins, P. J. Lundmark, E. C. Phillips, S. J. Rettig, J. E. Veltheer, *Organometallics* **1992**, 11, 2991−3003.
[25] A. Wlodarczyk, J. P. Maher, S. Coles, D. E. Hibbs, M. H. B. Hursthouse, K. M. A. Malik, *J. Chem. Soc., Dalton Trans.* **1997**, 2597−2605.
[26] T. R. Weaver, T. J. Meyer, S. A. Adeyemi, G. M. Brown, R. P. Eckber, W. E. Hatfield, E. C. Johnson, R. W. Murray, D. Untereker, *J. Am. Chem. Soc.* **1975**, 97, 3039−3048.
[27] Cambridge Structural Database, Version 2.3.7, **1998**. Cambridge Crystallographic Data Centre, Cambridge, England.
[28] J. S. Filippo, R. L. Grayson, H. J. Sniadoch, *Inorg. Chem.* **1976**, 15, 269−274.
[29] J. A. Baumann, T. J. Meyer, *Inorg. Chem.* **1980**, 19, 345−350.
[30] W. P. Griffith, *J. Chem. Soc. (A)* **1969**, 211−218.
[31] J. N. Burstyn, A. E. Yu, E. A. Dierks, B. K. Hawkins, J. H. Dawson, *Biochemistry* **1995**, 34, 5896−5903.
[32] L. J. Ignarro, *Seminars in Hematology* **1989**, 26, 63−76.
[33] J. S. Stamler, D. J. Singel, J. Loscalzo, *Science* **1992**, 258, 1898−1902.
[34] N. E. Le Brun, S. C. Andrews, G. R. Moore, A. J. Thomson, *Biochem. J.* **1997**, 326, 173−179.
[35] J. Springborg, P. C. Wilkins, R. G. Wilkins, *Acta Chem. Scand.* **1989**, 43, 967−974.
[36] D. E. Coufal, P. Tavares, A. S. Pererira, B. H. Hyunh, S. J. Lippard, *Biochemistry* **1999**, 38, 4504−453.
[37] V. M. Sellers, M. K. Johnson, H. A. Dailey, *Biochemistry* **1996**, 35, 2699−2704.
[38] M. W. Foster, J. A. Cowan, *J. Am. Chem. Soc.* **1999**, 121, 4093−4100.
[39] D. S. Bohle, C.-H. Hung, B. D. Smith, *Inorg. Chem.* **1998**, 37, 5798−5806.
[40] G. M. Sheldrick, SHELXTL, Version 5.03/Iris, Universtität Göttingen, **1994**.

Received February 2, 2000
[I00035]